Maciej Śniechowski,
Jacek Nizioł,
Wojciech Łużny

AGH University of Science and Technology, WFiIS,
al. Mickiewicza 30, 30-059 Kraków, Poland
e-mail: sniechowski@novell.ftj.agh.edu.pl

Structural Properties of Organometallic Thin Films Oriented by Corona Poling

Abstract
In this article, we review some results of structural studies of a novel series of donor–acceptor bis-alkynyl ruthenium chromophores in the form of thin films. At first, these thin films were oriented by a corona poling technique and were optically characterized using(Second and Third Harmonic Generation, respectively (SHG and THG). Next, the X-ray diffraction (XRD) technique was used to correlate the Nonlinear Optics (NLO) properties and directly observe the structural ordering of the studied materials. The last paragraph presents recent supramolecular modelling studies using molecular dynamics simulations. The used of organometallic films in textronic systems may be of the highest importance in order to achieve the possibility of creation micro-electro-optical sensors and circuits incorporated in textiles.

Key words: *nonlinear optics, SHG, THG, corona poling, XRD.*

Introduction

Organometallic materials have recently received considerable attention due to possible applications in nonlinear optics and quantum electronics [1]. The used of organometallic films in textronic systems also may be of the highest importance in order to achieve the possibility of creation micro-electro-optical sensors and circuits incorporated in textiles

It was shown that ruthenium derivative chromophores incorporated into the PMMA polymer matrix easily underwent optical poling [2]. This work is a joint study of the NLO and structural properties of a novel series of donor-acceptor bis-alkynyl ruthenium chromophores transformed into thin films. First, these thin films were oriented by a corona poling technique and were optically characterized using SHG and THG [3]. Next, the X-ray diffraction (XRD) technique was used to correlate the NLO properties and directly observe the structural order of the studied materials.

Materials

Organometallic complexes

The syntheses of alkynyl complexes (*trans*-[Ru(4-C≡CC_6H_4N=NC_6H_4-N(C_4H_9)$_2$)Cl(dppe)$_2$] (**A**), *trans*-[Ru(4-C≡CC_6H_4N=NC_6H_4-N(C_4H_9)$_2$)(4-C≡CC_6H_4CHO)(dppe)$_2$] (**B**) and *trans*-[Ru(4-C≡CC_6H_4N=NC_6H_4-N(C_4H_9)$_2$)(4-C≡CC_4H_2SCHO)(dppe)$_2$] (**C**)) were carried out according to previously reported procedures [4]. Bis-alkynyl ruthenium chromophores were asymmetrically functionalized around the ruthenium centre, as shown in ***Figure 1***.

The π-conjugated spacer, which consisted of an azo and an organometallic bis-alkynyl-ruthenium group, provided a long conjugation between the donor group (N,N-dibutylamine) and three different acceptors. A very important feature of these complexes was their ability of film formation through casting from the solution. This route was followed in the present study with dichloromethane as the solvent.

Experimental

Corona poling

Thin films prepared from the studied compounds were subjected to corona

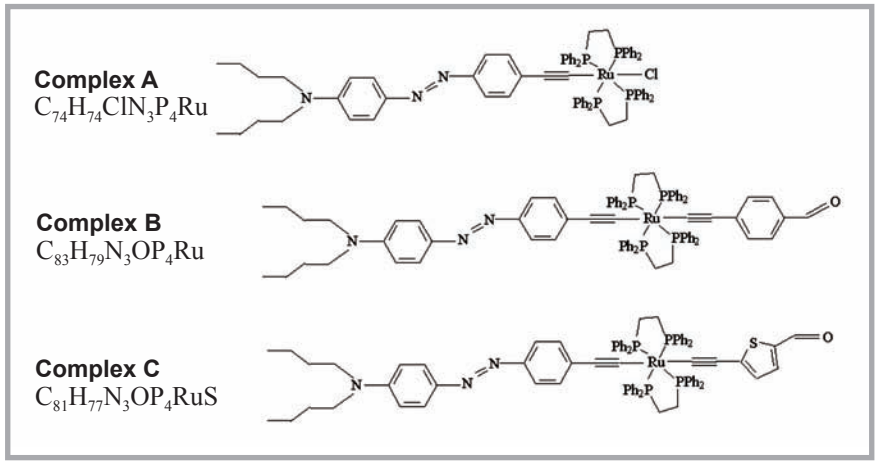

Figure 1. *Chemical structures of the studied organometallic complexes.*

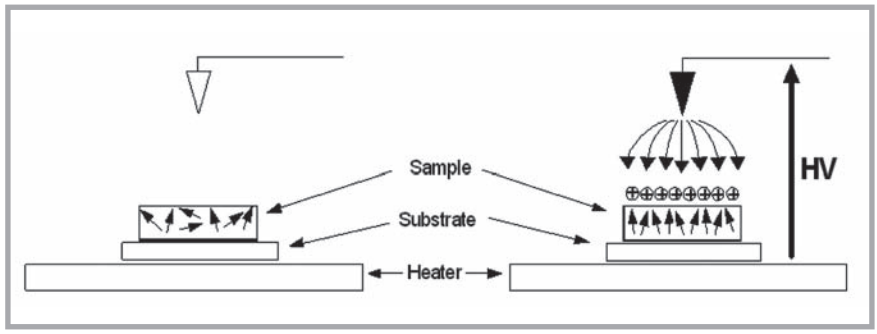

Figure 2. *Thin films made of the studied compounds were subjected to corona poling. This technique is commonly used for orienting NLO chromophores confined in an optically inert, transparent matrix. We used home-made apparatus, which enabled heating up to 180 °C and delivered 12 keV of static electric field.*

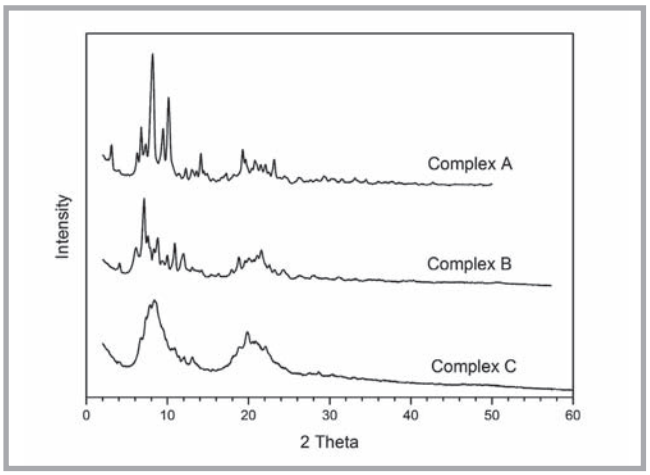

Figure 3. *WAXS profiles of powders A, B, C. Curves were shifted vertically for clarity.*

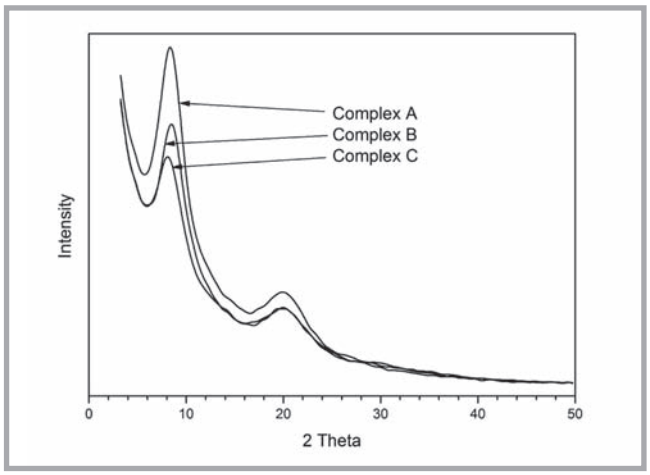

Figure 4. *WAXS profiles recorded for the thin films A, B, C.*

poling. This technique is commonly used for orienting the NLO chromophore confined in an optically inert, transparent matrix [4]. We used home-made apparatus, which enabled heating up to 180 °C and delivered 12 keV of static electric field. The samples were conditioned in these conditions for a given period then cooled down to room temperature. Finally, the field was turned off (see ***Figure 2,*** see page 89).

X-ray diffraction

Wide-angle X-ray diffraction (WAXS) measurements were carried out in the parallel beam reflection geometry and the classical Bragg-Brentano geometry using Cu Kα radiation (1.542 Å) [5]. The PanAlytical X'Pert PRO diffractometer was equipped with a parallel beam parabolic Göbel mirror to improve the scattering intensities from the film samples. The scan step varied from 0.05 to 0.1 (in 2θ) with counting times from 15 to 60 s per step. In general, raw data have to be folded with the instrumental resolution of the diffractometer. However, in our case, the broadening of peaks due to disordering is much larger than that of the instruments. We decided to use all the experimental curves as measured, just modified by a scaling factor accounting for the differences in size of the samples.

Results and discussion

The WAXS diffractograms obtained for the powders indicated differences in the crystallinity degree. The powders of A and B were partly ordered like typical molecular crystals and their coherence length neighboured c.a. 300 Å, whilst sample C was virtually amorphous (see ***Figure 3***). Once the powders had been transformed into thin films, the order disappeared (see ***Figure 4***). A first inspection of the patterns obtained for films revealed exclusively the presence of quasi-amorphous peaks. In addition, these diffraction patterns were almost identical for all three compounds; in other words, they did not depend on the acceptor substituent (Cl, benzene or thiophene). The observed differences in intensities were attributed to the statistics and the film thickness. All these diffraction patterns can be described as consisting of one somewhat sharp reflection at a smaller 2θ value (2θ = 8.5°) and a broader one with an intensity maximum centred at 2θ = 20°, both imposed on an exponential background. The positions of these two peaks at 2θ = 8.5° and 2θ = 20° correspond to ordering repeat distances d = 10.5 Å and 4.5 Å, respectively. The coherence length (average dimensions of ordered regions) estimated from the broadening of the first reflection maxima is around 30Å – the order is very poor – at a distance comparable to the molecule dimensions.

Two-dimensional scattering patterns were obtained using a Eulerian Cradle. The rotation of the sample around the beam axis gives direct access to the full range of **q** vector (scattering vector, where $|q| = 4\pi \sin\theta / \lambda$, where λ-X-ray wavelength) orientations with respect to the film surface. In others words, the whole range of crystallographic planes present in the sample can be observed (not only those oriented parallel to the sample plane). The strong anisotropy is observed between the film plane q_xy and the scattering vector parallel to the film orientations q_z. Instead of Debye-like circles (as in polycrystalline samples), well-isolated regions of maxima can be distinguished (see ***Figures 5*** and ***6***). This is a fingerprint of the strong anisotropy of the supramolecular structure present in the studied samples. Another interesting observation is the strong anisotropy of a broad amorphous background (see ***Figure 5***) (which will be discussed elsewhere). As a result of a series of experiments, performed un-

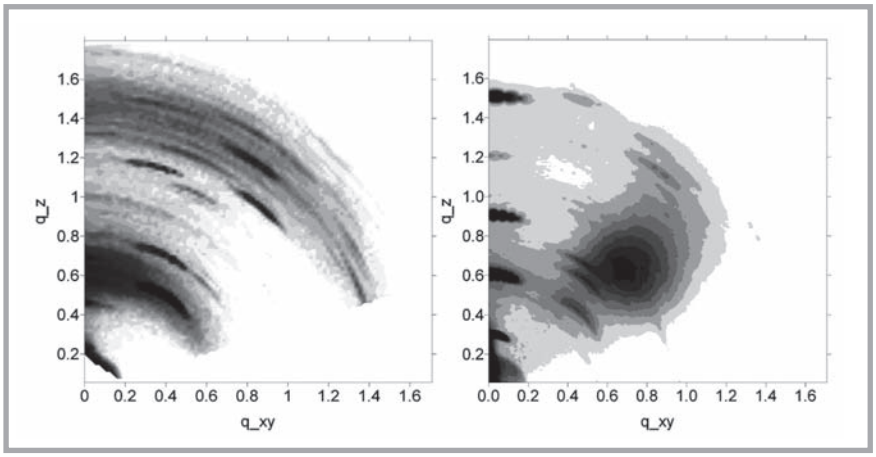

Figure 5. *2D X-ray scattering patterns of A (left) and B (right); q_z and q_xy stand for perpendicular to the plane and in-plane components of the scattering vector, respectively.*

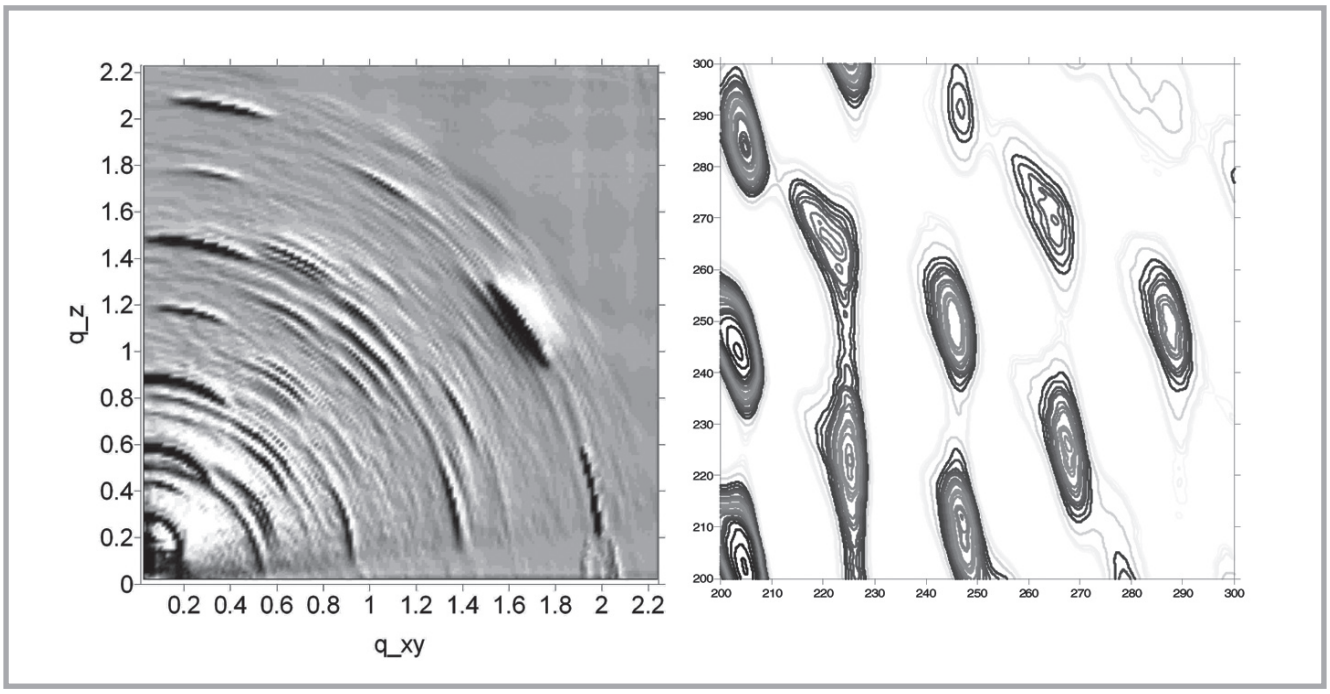

Figure 6. *2D X-ray scattering pattern of highly oriented film B (left) and the Patterson function calculated using this scattering pattern (right).*

der varied conditions, we found that the substantial 2D patterns observed for films prepared from compounds A and B remained similar. The film of B was always better oriented than the film of A, despite the degree of crystallinity invoked by the given treatment procedure. The result is consistent with the measurements of SHG collected in ***Table 1***. The second-order nonlinear optical susceptibility measured from the better oriented film of B is significantly higher compared with the result obtained for films of A.

Structure modelling

The procedure of modelling the supramolecular structure (the order of the chromophore molecules in the system) consisted of the following steps. First, the individual molecules were built and geometrically optimized (see ***Figure 7***). An isolated, such optimized molecule was put into a cubic periodic box that was then geometrically optimized (cell dimension and angles) by an energy minimization algorithm. Optimized triclinic periodic boxes ("crystal unit cells") were used to build supercells consisting of 8, 16 or 64 independent molecules in a periodic condition. Bigger supercells were introduced to reproduce better the statistical disorder of the molecules in a real physical structure. The stability of these models (supercells) was examined by 100 ps long molecular dynamic simulation using the NPT ensemble (constant pressure, constant temperature). The last frame of MD simulation is shown in ***Figure 8***. Direct inspection of the supramolecular structure modelling shows that the chromophore packing is driven by the geometry of the huge spacer (transmitter) (see ***Figure 7***) with heavy ruthenium atoms forming a pseudo-hexagonal lattice. The chromophore packing obtained from simulations was examined more quantitatively compared with the Patterson

Table 1. *Comparison (before and after corona poling) of second-order nonlinear optical susceptibility (with pp-polarization) and third-order nonlinear optical susceptibility (with ss-polarization) for the complexes A and B (for technical reasons, the thin film made of complex C didn't undergo SHG and THG measurements).*

Compounds	Corona poling	$\chi_{eff}^{<2>}$ pm/V	$\chi_{elec}^{<3>}$ (× 10^{-20}), m^2/V^2
A	Before	0.11	1.95
	After	0.23	1.96
B	Before	0.17	3.01
	After (highly oriented)	1.02	2.98

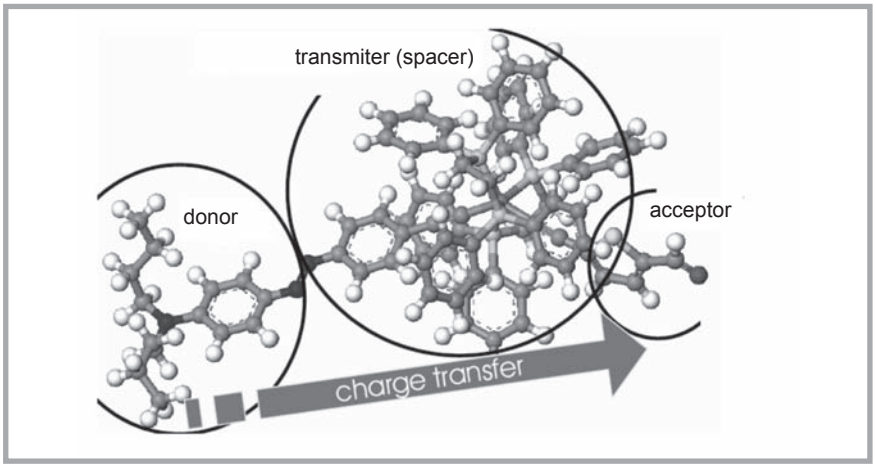

Figure 7. *Molecule design (energy minimization optimized structure): transition metal s-acetylide complexes have an almost linear M-CoC-R structure and give rise to an efficient electronic coupling between the metal and the remote groups through the p-conjugated path. Ruthenium-alkynyl fragment is a powerful donor that can compete with the strongest organic donors.*

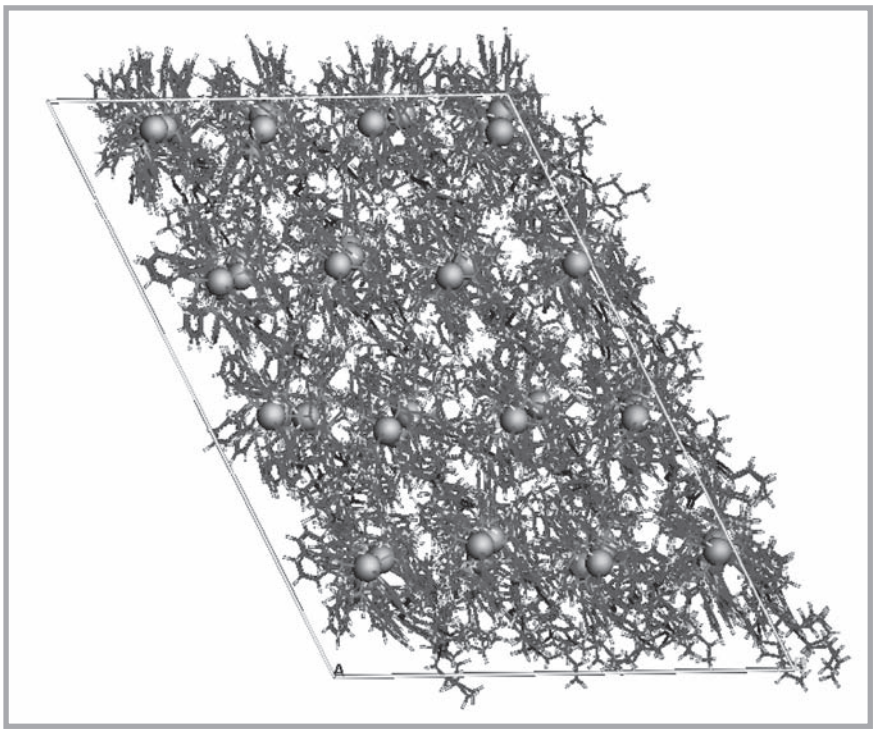

Figure 8. *Simulated supramolecular structure of organometallic complex C, supercells (periodic box) consisting of 64 independent molecules. (The larger grey spheres represent the Ruthenium sites in each molecule).*

function calculated from the experimental data (see ***Figure 6***).

The Patterson function map (representing the probability distribution of inter-atomic distances) was calculated starting from a 2D map of recorded diffraction intensity. This can be interpreted in a certain manner as the distribution electron density in the real space of the crystal.

$$P(u) = 1/V \cdot \sum I_{\exp}(q) \cdot \exp(-2\pi uq)$$

– Patterson function where: q-> (q_z,q_{xy}) – reciprocal space vectors; u-> (u_z,u_{xy}) – real space vectors.

The calculated experimental 2D Patterson function map (see ***Figure 6***) clearly evidenced the pseudohexagonal packing of chromophores similar to that obtained as a result of the molecular dynamics simulation.

Conclusions

We have shown that free-standing films of a new family of functionalized alkynyl ruthenium complexes, subjected to an elevated electric field at a temperature close to the glass transition temperature, significantly changed their structural properties. In addition, corona poling induced relatively high structural anisotropy of the films. It was also observed that the magnitude of second-order nonlinear optical susceptibility $\chi_{eff}^{<2>}$ could be correlated with the directly observed chromophore supramolecular structure and orientation induced by corona poling.

Acknowledgements

This work was partly supported by research grant no. 3 T08E 083 30 from the Polish Ministry of Science and Higher Education.

References

1. *A. Migalska-Zalas, J. Luc, B. Sahraoui and I. V. Kityk, Optical Materials, Vol. 28, 1147-1151 (2006).*
2. *A. Migalska-Zalas, Z. Sofiani, B. Sahraoui, I.V. Kityk, S. Tkaczyk, V. Yuvshenko, J.L. Fillaut, J. Perruchon and T.J.J. Muller, J. Phys. Chem. B, Vol. 108, 14942-14947 (2004).*
3. *F. Kajzar, P-A. Chollet in Poled Polymers and their Applications to SHG and EO Devices, Gordon & Breach Science Publishers (1997).*
4. *J.-L. Fillaut, J. Perruchon, P. Blanchard, J. Roncali, S. Golhen, M. Allain, A. Migalska-Zalas, I.V. Kityk and B. Sahraoui, Organometallics, Vol. 24, 687-695 (2005).*
5. *V. Holy, U. Pietsch and T. Baumbach, High Resolution X-Ray Scattering from Thin Films and Multilayers, Springer, 2nd edition (2004).*

Received 23.05.2008 Reviewed 9.12.2008